Precision laser spectroscopy of the $2\,^1S_0 - 3\,^1D_2$ two-photon transition in ^{3}He

Yi-Jan Huang,[1] Yu-Chan Guan,[1] Jin-Long Peng,[2] Jow-Tsong Shy,[1,3,*] and Li-Bang Wang[3,†]

[1]*Institute of Photonics Technologies, National Tsing Hua University, Hsinchu 30013, Taiwan*

[2]*Center for Measurement Standards, Industrial Technology Research Institute, Hsinchu 30011, Taiwan*

[3]*Department of Physics, National Tsing Hua University, Hsinchu 30013, Taiwan*

(Received 19 December 2019; accepted 4 May 2020; published 4 June 2020)

We have measured the absolute frequency of the $2\,^1S_0 - 3\,^1D_2$ two-photon transitions in ^{3}He at 1009 nm based on a cesium frequency standard through an optical frequency comb. The measured frequencies are 594 384 961.072(19) MHz for the $2\,^1S_{0,1/2} - 3\,^1D_{2,5/2}$ transition and 594 384 821.209(15) MHz for the $2\,^1S_{0,1/2} - 3\,^1D_{2,3/2}$ transition with relative uncertainties of 2.5×10^{-11} and 3.9×10^{-11}, respectively. The determination of the $2\,^1S_0 - 3\,^1D_2$ two-photon transition frequency, without hyperfine effect, in ^{3}He is 594 384 761.556(12) MHz. The deduced isotope shift between ^{3}He and ^{4}He is 29.530246(18) GHz. The difference of the squares of the nuclear charge radii is deduced to be 1.059(25) fm^2. Finally, by combining other precise measured transitions, we are able to derive the $3\,^3D_1 - 3\,^1D_2$ separation in ^{3}He to be 101 058 203(56) kHz, which is an improvement by a factor of 89 compared to previous work.

DOI: 10.1103/PhysRevA.101.062507

I. INTRODUCTION

Absolute frequency measurements in atomic helium transitions are crucial for the test of many-body quantum electrodynamics (QED) atomic calculations [1–5]. It can be sensitive to the nuclear size effect on the accuracy of 10^{-2}–10^{-4} which are enough to compare with theoretical calculation [6]. For example, it is of particular interest in the determination of the proton charge radius [7–10]. The accurate value of the proton radius allows theorists to improve the important determination of the Rydberg constant. Recently, a result [11] from atomic hydrogen shows an agreement with the values of the proton radius from muonic hydrogen, but being inconsistent with previous measurements of the same type. However, this new result calls for more studies [8,12] in the physics beyond the standard model.

Muonic helium spectroscopy can provide quite precise values of nuclear charge radii [13,14]. In atomic helium spectroscopy, the difference of the squares of the nuclear charge radii (δR^2) is a kind of corresponding measurement [5,6,15–20] for the discussion of the nuclear charge radius. For instance, the δR^2 of ^{3}He and ^{4}He can be derived from the isotope shifts of ^{3}He and ^{4}He in helium spectroscopy. Through the isotope shift, the uncertainties of high-order QED terms can be canceled in the same transitions of the isotopes of ^{3}He and ^{4}He, so by comparing the results of the atomic and muonic helium spectroscopy could provide an alternative test for the yet unknown $\alpha^7 m$ correction of QED term. In current comparison of the δR^2 of ^{3}He and ^{4}He, there is a 5σ disagreement among several precise measurements [14,18–24] involving the laser experiments and electronic scattering experiments.

Furthermore, although the He spectroscopy has been greatly improved, the spectroscopy of ^{3}He transitions involving $3D$ singlet states remain rare measurements. With respect to the singlet-triplet mixing in nD state, according to the theoretical report [1], their results only agree with the experimental measurements for $n = 4$, 5, and 6. A discrepancy was found for $n = 3$ according to an earlier paper [25] that presented measurements of the separations between the $n\,^3D$ and $n\,^1D$ states in ^{3}He. A discrepancy between the theoretical and experimental determination remains at 37 MHz for the $3\,^1D - 3\,^3D$ separation in ^{3}He. Likewise, there are seldom measurements resolving hyperfine structures of ^{3}He except for the $2\,^3S_1 - 2\,^3P_j$ and $2\,^3S_1 - 2\,^1S_0$ transitions. Recently, the $2\,^3P - 3\,^3D_1$ transitions [26] in triplet states of ^{3}He including hyperfine splitting have been measured precisely. Thus, we can derive the separation of the $3\,^1D_2 - 3\,^3D_1$ by measuring the $2\,^1S_0 - 3\,^1D_2$ two-photon transition.

In our previous work [27] we have already measured the $2\,^1S_0 - 3\,^1D_2$ two-photon transition in ^{4}He. As a continuous work, we are going to report the frequency measurements of the $2\,^1S_0 - 3\,^1D_2$ two-photon transitions in ^{3}He at 1009 nm. First, by combining our results in ^{4}He and ^{3}He, the isotope shift of the $2\,^1S_0 - 3\,^1D_2$ two-photon transition can be determined with the uncertainties reaching less than 20 kHz. We can derive the δR^2 of ^{3}He and ^{4}He with the relative accuracy of 10^{-2}, by adopting the coefficients and our results of the isotope shift into the formula referred to in calculation [28]. Second, we measure the hyperfine structure of the $3\,^1D_{2,5/2}$ and $3\,^1D_{2,3/2}$ states in ^{3}He, and reach a precision of 7 kHz. Last, the $3\,^1D_2 - 3\,^3D_1$ fine structure separation in ^{3}He can be determined with an accuracy of 56 kHz, in combination with other measurements [18,22,26] and the hyperfine corrections [1], which improves the precedent result by a factor of 89,

*shy@phys.nthu.edu.tw

†lbwang@phys.nthu.edu.tw

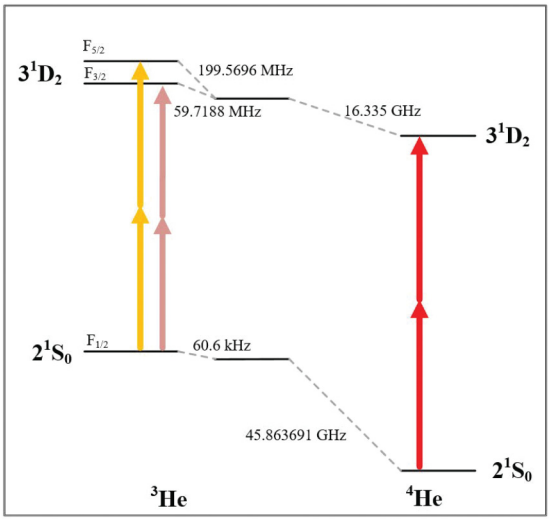

FIG. 1. The energy levels diagram of the $2\,^1S_0$–$3\,^1D_2$ in ^{3}He and ^{4}He. Due to the nuclear spin of 1/2, the $3\,^1D_2$ state of ^{3}He splits into two hyperfine states $3\,^1D_{2,5/2}$ and $3\,^1D_{2,3/2}$, which are separated by ∼140 MHz. The isotope shifts of this transition is ∼29.5 GHz. The values are taken from Ref. [1].

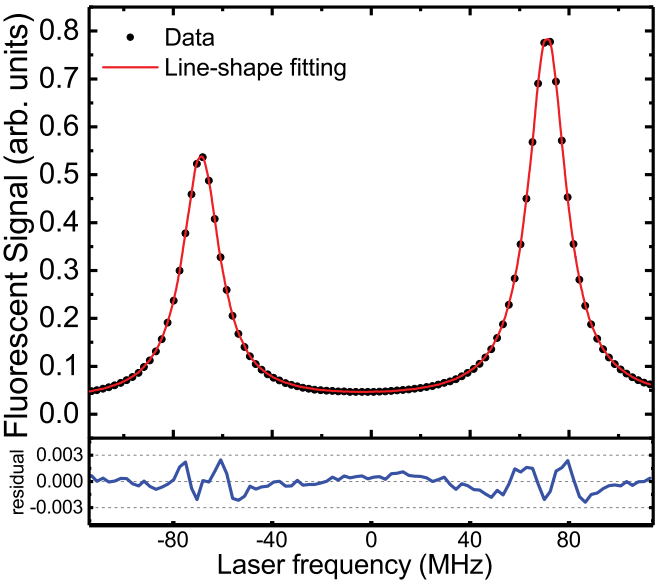

FIG. 2. The typical spectrum of the $2\,^1S_0$–$3\,^1D_2$ two-photon transitions in ^{3}He. The red line is the fitting profile that is the sum of the two independent Lorentzian functions and a line function. The blue line in the lower panel is the residuals of the fitting, where the ratio of signal to residual is more than 200. The zero of the frequency axis is 297 192 445 MHz.

and the result is precise enough to be compared with the theoretical calculation (28 kHz).

II. EXPERIMENT

The energy levels diagram of the $2\,^1S_0$–$3\,^1D_2$ in ^{3}He and ^{4}He are shown in Fig. 1. Due to the nuclear spin of 1/2 in ^{3}He, the $3\,^1D_2$ state is split into two hyperfine states, $3\,^1D_{2,5/2}$ and $3\,^1D_{2,3/2}$. The two hyperfine transitions are separated by approximately 140 MHz. However, the natural linewidth of state ($2\,^1P_1$) is up to 300 MHz due to the short lifetime (0.551 ns) [29]. To resolve the hyperfine splitting, this would give challenges by means of the one-photon $2P$–$3D$ transition, but the Doppler-free two-photon spectroscopy can provide the natural linewidth of only 10 MHz limited by the upper state ($3\,^1D_2$).

The experimental setup of two-photon spectroscopy is similar to the one used in our previous work of ^{4}He [27]. From the previous experience, the discharge of helium is so sensitive to the impurities that we always ensure the purity (>98%) of the ^{3}He before starting the spectral measurements. The ^{3}He atoms in $2\,^1S_0$ excited state are also prepared by the radio frequency (rf) discharge, and are driven by two-photon transition to the $3\,^1D_2$ state using the power-enhanced configurations and a single-mode external cavity diode laser (ECDL) as the 1009 nm light source.

The absolute frequency metrology is based upon the optical frequency comb (OFC) system [30] which is stabilized on a cesium frequency standard with a stability of 7.3×10^{-12} at 1 s. In order to scan over the two hyperfine components at one time, we used some effort to improve the stabilities of locking systems so that we can set the frequency scanning range of ECDL to 125 MHz (250 MHz at spectrum) that are 4 times larger than in the previous work of ^{4}He, which is very close to our scanning limit that is the half repetition frequency of OFC.

The two-photon spectroscopy of the $2\,^1S_0$–$3\,^1D_2$ transitions in ^{3}He is demonstrated in Fig. 2. The first smaller peak is the $2\,^1S_0$–$3\,^1D_{2,3/2}$ transition. Another is the $2\,^1S_0$–$3\,^1D_{2,5/2}$ transition. Comparing to the previous measurements [27] in ^{4}He, this time we apply the 4 times larger scanning range to cover two peaks at a single scan. The optical frequency spacing between each two points is 2.38 MHz that is driven in steps by tuning the repetition rate of the OFC which the ECDL is locked to. The data of both frequency and spectral signal are acquired with an integration time of 4 s after a waiting time of 1 s for all the locked systems being stable. So, the overall scanning process is very slowly with 5 s per point. To obtain the center frequencies and spectral widths, the measurements are fitted by a modified function that includes independent Lorentzian functions, quantum interference terms, and a linear background. In Fig. 2 the ratio of signal to residual is more than 200. Besides, with the same experimental variables, the measurements are repeated ten times, and we use a constant fitting to the obtained center frequencies as shown in Fig. 3. The one-standard error (half red zone) is less than 20 kHz.

III. RESULTS AND ANALYSIS

For the investigation of the pressure and power shifts, we systematically varied pressure and intracavity power, and show the center frequencies of $2\,^1S_0$–$3\,^1D_2$ two-photon transitions in Fig. 4. To the best of our knowledge, the most possible reason for the power correction is AC-Stark shift. At the first step we varied the interacted optical power from 10 to 16 W at one fixed pressure. A constant fitting to ten measurements with the same condition presents one experimental point. The experimental data distribution and AC-Stark theory both suggested to us to use a linear extrapolation to the power

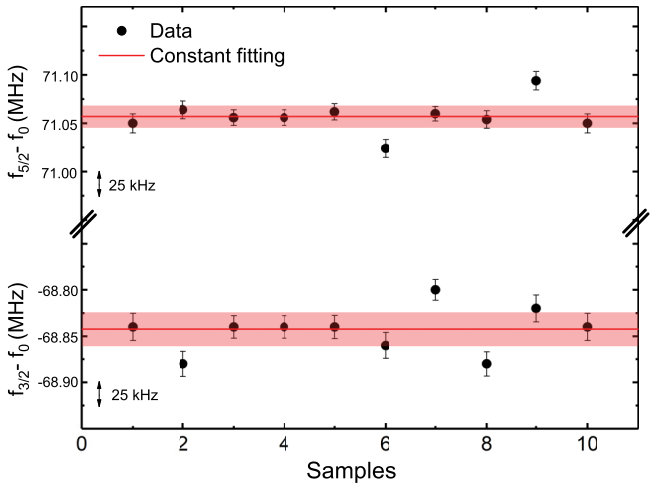

FIG. 3. A constant fitting to the ten measurements of the $2\,^1S_0 - 3\,^1D_2$ transitions to present one of the points in Figs. 4(a) and 4(c), where f_0 is 297 192 445 MHz. The error bar on each point in this figure shows the standard deviation of the fitting when determining the center frequency of a spectrum. Under the same experimental condition, the uncertainty of a constant fitting (half red zone) is always less than 20 kHz.

variation. After repeating the measurements to other pressures, we can obtain Figs. 4(a) and 4(c), where each color line means the center frequencies measured at pressures from 30 to 192 mTorr while varying the interacted optical power from 10 to 16 W.

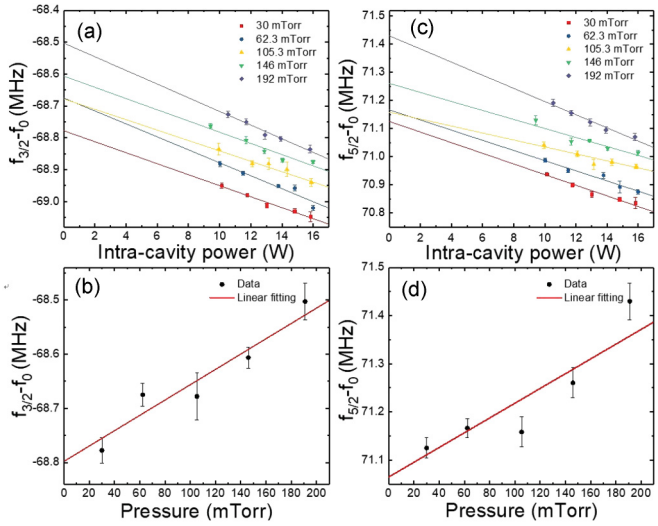

FIG. 4. (a) and (c) Records of the spectrum fitting of the center frequencies at one of the pressures from 30 to 192 mTorr while varying the interacted optical power from 10 to 16 W corresponding to the $2\,^1S_{0,1/2} - 3\,^1D_{2,3/2}$ transition and the $2\,^1S_{0,1/2} - 3\,^1D_{2,5/2}$ transition, respectively, where f_0 is 297 192 445 MHz. The zero-power frequency from (a) and (c) at different pressures are plotted in (b) and (d) to obtain the frequency in the zero power and pressure. The coefficients of the power shift are averaged to be −9.30(42) kHz/W in the $2\,^1S_{0,1/2} - 3\,^1D_{2,5/2}$ transition and −8.80(72) kHz/W in the $2\,^1S_{0,1/2} - 3\,^1D_{2,3/2}$ transition. Besides, the coefficients of the pressure shift are 0.70(10) and 0.77(11) kHz/mTorr, respectively.

The coefficients of the power shift are averaged to be −9.30(42) kHz/W in the $2\,^1S_{0,1/2} - 3\,^1D_{2,5/2}$ transition and −8.80(72) kHz/W in the $2\,^1S_{0,1/2} - 3\,^1D_{2,3/2}$ transition. In the experimental sequences, the power variation was studied at one fixed pressure first, so we use the free parameter to the slopes of each linear fitting instead of a global fitting (a shared slope) for all data, though the slopes are located within the range of one standard deviation of mean. After using the linear extrapolation of the power variation, the zero-power frequency at different pressures are plotted, and shown in Figs. 4(b) and 4(d). The extrapolated coefficients of the pressure shift are 0.70(10) kHz/mTorr in the $2\,^1S_{0,1/2} - 3\,^1D_{2,5/2}$ and 0.77(11) kHz/mTorr in the $2\,^1S_{0,1/2} - 3\,^1D_{2,3/2}$ transition.

In every spectrum the optical power transmitted through one of the mirrors of power-enhanced cavity were recorded, and the changes were ensured to be less than 2.5% with an integration time of 0.5 s. In order to be cautious, we took 5% power uncertainty into account (including the measuring error of the power meter, Thorlabs 302C). In addition, the changes of the fixed pressure were less than 1% over 2 weeks even with rf discharge on, and 1% pressure uncertainty is adopted to the error budget.

In the experiment the range of gas temperature with the rf discharge is estimated to be 300–400 K. Accordingly, the second order Doppler shift is deduced to be 9.6(1.0) kHz. For the estimation of the Zeeman effect, we have measured the magnetic field <1 mG. Thus, the maximum Zeeman shift for the circularly polarized configuration is 1.4 kHz. However, our configuration, with the cavity and Brewster windows inside, ideally provides a pure linear polarization of light to interact with atoms. We still carefully assume 1 kHz for the uncertainty of the Zeeman effect.

To estimate the possible frequency shifts of the quantum interference effects, we adopt the method by Li *et al.* [34], in which a precision of 1 kHz is achieved in the $D1$ line of lithium. A fitting function is applied to take the quantum interference effect into account. There are only two close hyperfine transitions in our case. Thus, the Lorentzian functions with the quantum interference terms have the form [34,35]

$$f(w) = \frac{g_1}{(w-w_1)^2 + \left(\frac{\Gamma}{2}\right)} + \frac{g_2}{(w-w_2)^2 + \left(\frac{\Gamma}{2}\right)} + 2\mathrm{Re}\left\{\frac{g_{12}}{\left[w - w_1 + i\left(\frac{\Gamma}{2}\right)\right]\left[w - w_2 - i\left(\frac{\Gamma}{2}\right)\right]} + \frac{g_{21}}{\left[w - w_2 + i\left(\frac{\Gamma}{2}\right)\right]\left[w - w_1 - i\left(\frac{\Gamma}{2}\right)\right]}\right\},$$

where the w_1 and w_2 are the centers of transition frequencies, Γ is the linewidth that can be deduced from the lifetime of state, g_1, g_2 are determined by the dipole moments of the transitions, and g_{12}, g_{21} mean the interaction coefficients. The last two terms are from the close hyperfine interaction.

We have included the quantum interference terms in the fitting program. However, in different experimental conditions, the differences for center frequency determination are always smaller than 2 kHz between the original Lorentz function and the modified function. The discrepancy is much smaller than the uncertainty of the 10-kHz level. The quantum interference

TABLE I. Error budgets of the $2\,^1S_{0,1/2}-3\,^1D_{2,3/2}$ two-photon transition (unit: kHz).

Items	Corrections	Uncertainty
Statistics		13
Second-order Doppler effect	+9.6	1
Zeeman effect		1
Quantum interference		2
OFC accuracy[a]		4
Offset locking[b]		<2
Power measurement		<7
Pressure measurement		<1
Overall	+9.6	15

[a]Multiple a factor of 2.
[b]The frequency locking of the ECDL and OFC.

effects are quite different in various experimental setups. In our case of the two-photon transition with a hot gas cell, it could be different from other experiments and may require further investigation with much higher precision. Carefully we present the quantum interference effects by adding additional uncertainties of 2 kHz into the error budget.

After considering pressure shifts, power shifts, the second order Doppler shifts, and the quantum interference effects, the absolute frequencies are 594 384 961.074(19) ($f_{5/2}$) and 594 384 821.212(15) MHz ($f_{3/2}$). Taking $f_{3/2}$ as an example, the experimental uncertainties are listed in Table I.

To obtain the absolute frequency without hyperfine effects, the two transitions are subtracted respectively by the referred hyperfine shifts (HFS) [1], 199.5696 MHz for $3\,^1D_{2,5/2}$, 59.7188 MHz for $3\,^1D_{2,3/2}$, and 0.0606 MHz for $2\,^1S_{0,1/2}$ with a theoretical uncertainty of 0.0001 MHz. The $2\,^1S_0-3\,^1D_2$ transition frequency in ^{3}He without hyperfine effects is 594 384 761.558(12) MHz, which is in a really good agreement with the theoretical calculation [1] 594 384 761.5(5.0) MHz.

Using the determination of the $2\,^1S_0-3\,^1D_2$ transition [27] in ^{4}He, 594 414 291.803(13) MHz, we obtain the isotope shift of 29.530245(18) GHz. Substituting the isotope shift into a formula with corresponding C coefficients [1], the δR^2 is deduced to be 1.059(25) fm^2. This work's centroid value agree well with electronic scattering determination [1.066(6) fm^2]. The comparison of the recent determinations of δR^2 is shown in Fig. 7, where the determinations of δR^2 are from the measurements [18,19,22–24] that were improved by the updated theoretical values [5,6], and including the latest electronic scattering determination [14]. Recently, the work [19] presented good measurements of the $2\,^3S_1-2\,^3P$ transitions with sub-kHz precision and, however, mentioned the disagreement between the determinations of δR^2. In our case, in the derivation of the δR^2, the difference of the C coefficients between $2\,^1S_0$ and $3\,^1D_2$ is much smaller than between the $2\,^3S_1$ and $2\,^3P$ states, which leads to less accuracy to determine δR^2 from our result. However, there are still important features in our measurement. It is the only precise measurement deriving the δR^2 from the transitions of the singlet state, and given the level of 10 kHz precision.

Although high order corrections of QED still limit the precision in the calculation of the $2S$ states, there are two

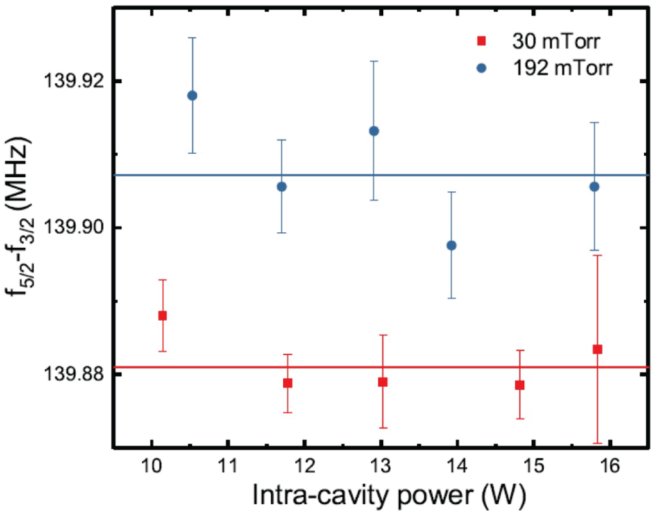

FIG. 5. The demonstration of two constant fitting of the hyperfine $3\,^1D_{2,5/2}-3\,^1D_{2,3/2}$ separation in both ends of the pressure condition to show the power variation. Under the same pressure with different power conditions, the uncertainty of the constant fitting is always less than 10 kHz.

alternative comparisons to test our result. One is to use the comparison of the hyperfine shifts. We picked up the separations of the two spectral peaks in the fitting before any correction, and considered again pressure and power shifts for the separation. With respect to power variation, there are no significant differences, and the distribution examples are shown in Fig. 5. The result can be reasonably understood since the closed two hyperfine transitions carry the near AC-Stark shifts. Therefore, we use a constant fitting to the separation versus the varied optical power in a certain fixed pressure, and repeating it when changing the next pressure condition.

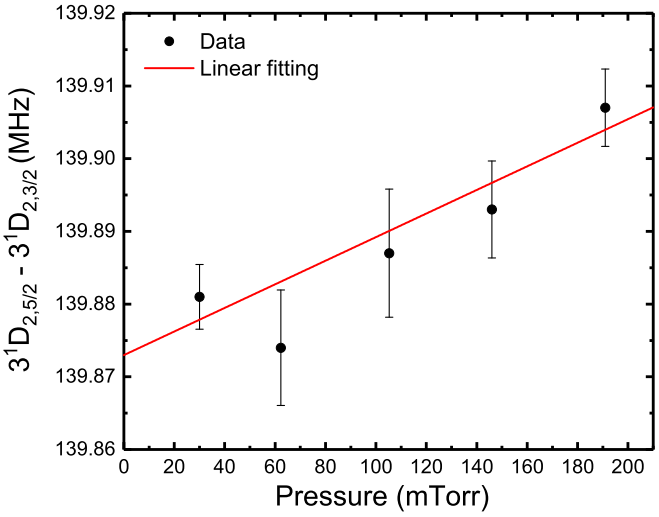

FIG. 6. The linear extrapolation of the hyperfine $3\,^1D_{2,5/2}-3\,^1D_{2,3/2}$ separation. In the figure each point is obtained from the value of the constant fitting at different pressures in Fig. 5. The pressure shift coefficient is 0.16(3) kHz/mTorr. After pressure correction, the hyperfine $3\,^1D_{2,5/2}-3\,^1D_{2,3/2}$ separation is determined to be 139.873(7) MHz.

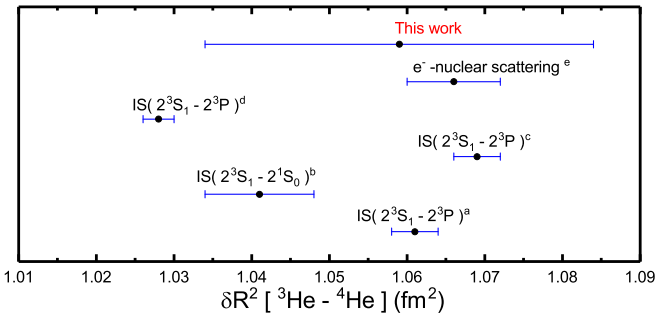

FIG. 7. The comparison of the determination of the δR^2 from other measurements and our work. (a) Shiner *et al.* [5,21]. (b) Rengelink *et al.* [20] and van Rooij *et al.* [22]. (c) Cancio Pastor *et al.* [5,18,23,24]. (d) Zheng *et al.* [19]. (e) I. Sick [5,14].

A linear extrapolation of the pressure dependence of the hyperfine separation is shown in Fig. 6. The pressure coefficient is 0.16(3) kHz/mTorr. Finally, the hyperfine separation is determined to be 139.873(7) MHz. Although there is a difference (11 kHz) between this determination and our above transition frequency determination [$f_{5/2}$-$f_{3/2}$, 139.862(24) MHz], they still agree well with each other. Ideally, the direct measurements of hyperfine separation should have better accuracy, because some factors are sensitive to absolute frequency measurements but insensitive to the separation measurements, such as, the jitter of the locked laser frequency, the fluctuation of intracavity power, and even some environment factors. For example, the separation become insensitive to intracavity power shown in Fig. 5 thanks to the synchronous AC-stark shifts of the two hyperfine states. However, if comparing to the theoretical calculation [1] 139.8508(2) MHz, we found a larger discrepancy of 3.2σ (22 kHz) between our result and the theoretical calculation.

Another comparison is to use the fine structure of $3D$ states. The determination of the $3\,^3D_1$–$3\,^1D_2$ separation in ^{3}He can be derived by combining the most precise measurements of the $2\,^3S_1$–$2\,^1S_0$ [22], $2\,^3S_1$–$2\,^3P$ [18], and $2\,^3P$–$3\,^3D_1$ [26] transitions in ^{3}He, corrections of HFS [1], and our results. Finally, the absolute frequency of the $3\,^3D_1$–$3\,^1D_2$ separation in ^{3}He is deduced to be 101 058.205(56) MHz, which is obviously smaller than the theoretical calculation [1] of 101 058.310(28) MHz by 2σ (105 kHz) shown in Table II. Moreover, the result [27] of the separation in the ^{4}He was reported by the similar deviation that is also smaller than the theoretical calculation [1] by 2σ (86 kHz). The latest new calculation for $3D$ states had been reported in [31], which presented the new calculation of the $3\,^3D_1$–$3\,^1D_2$ separation for ^{4}He. The latest experimental determinations of the $2S$ and $2P$ states are using the theoretical ionization energy of the $3D$ states, but some recent reports [19,26,32,33] pointed out the discrepancies between their results and theoretical calculations. Therefore, we believe there are still some quantum interest in the $3\,^3D_1$–$3\,^1D_2$ separation such as the mixing ratio of $3\,^3D$ and $3\,^1D$ states. In our result, both ^{3}He and ^{4}He measurements presented the similar deviation to the theoretical calculation.

TABLE II. The frequency comparison of the $3\,^3D_1$–$3\,^1D_2$ separation (unit MHz).

	Experiment	Theoretical calc.	Δ
^{4}He	101 143.943 (31)[a]	101 144.029 (23)[b]	−0.086
^{3}He	101 058.205(56)[c]	101 058.310(28)[d]	−0.105

[a]In combination with Refs. [19,20,26] and our previous work [27].
[b]Reference [31].
[c]In combination with Refs. [1,18,22,26] and this work.
[d]Reference [1].

IV. SUMMARY

We have measured the absolute frequencies of the $2\,^1S_0$–$3\,^1D_2$ two-photon transitions in ^{3}He with a precision of less than 20 kHz. Consequently, we have first shown the hyperfine structure of the $3\,^1D_2$ state. Furthermore, by combining our previous determination [27] in ^{4}He, we successfully provide an independent test for the determination of the δR^2 deriving from the isotope shift of the ^{3}He and ^{4}He in singlet states. Last but not least, the $3\,^3D_1$–$3\,^1D_2$ separation in ^{3}He is deduced precisely and improved by nearly two orders of magnitude. In future work it would be worthwhile to perform measurements to higher states from the $2S$ or $2P$ states, since most frequency measurements in low-lying states of helium use the theoretical value of the $3D$ states as a base for comparison of theory and experiment. In addition, the $n > 3$ states have been calculated more precisely, even reaching sub-kHz.

ACKNOWLEDGMENTS

We thank Chunghwa Telecom Laboratory for lending us a cesium clock. This project is supported by the Ministry of Science and Technology and the Ministry of Education of Taiwan. L.-B.W. acknowledges support from Kenda Foundation as a Golden-Jade fellow.

[1] D. C. Morton, Q. Wu, and G. W. Drake, Can. J. Phys. **84**, 83 (2006).
[2] G. W. Drake and Z.-C. Yan, Can. J. Phys. **86**, 45 (2008).
[3] Z. Pei-Pei, Z. Zhen-Xiang, Y. Zong-Chao, and S. Ting-Yun, Chin. Phys. B **24**, 033101 (2015).
[4] V. A. Yerokhin and K. Pachucki, Phys. Rev. A **81**, 022507 (2010).
[5] K. Pachucki, V. Patkóš, and V. A. Yerokhin, Phys. Rev. A **95**, 062510 (2017).
[6] K. Pachucki and V. Yerokhin, J. Phys. Chem. Ref. Data **44**, 031206 (2015).
[7] R. Pohl, A. Antognini, F. Nez, F. D. Amaro, F. Biraben, J. M. Cardoso, D. S. Covita, A. Dax, S. Dhawan, L. M. Fernandes *et al.*, Nature (London) **466**, 213 (2010).

[8] R. Pohl, R. Gilman, G. A. Miller, and K. Pachucki, Annu. Rev. Nucl. Part. Sci. **63**, 175 (2013).
[9] A. Antognini, F. Biraben, J. Cardoso, D. Covita, A. Dax, L. Fernandes, A. Gouvea, T. Graf, T. W. Hänsch, M. Hildebrandt *et al.*, Can. J. Phys. **89**, 47 (2011).
[10] C. E. Carlson, M. Gorchtein, and M. Vanderhaeghen, Phys. Rev. A **95**, 012506 (2017).
[11] A. Beyer, L. Maisenbacher, A. Matveev, R. Pohl, K. Khabarova, A. Grinin, T. Lamour, D. C. Yost, T. W. Hänsch, N. Kolachevsky *et al.*, Science **358**, 79 (2017).
[12] F. Ficek, D. F. J. Kimball, M. G. Kozlov, N. Leefer, S. Pustelny, and D. Budker, Phys. Rev. A **95**, 032505 (2017).
[13] E. Borie and G. A. Rinker, Phys. Rev. A **18**, 324 (1978).
[14] I. Sick, Phys. Rev. C **90**, 064002 (2014).
[15] W. Lichten, D. Shiner, and Z.-X. Zhou, Phys. Rev. A **43**, 1663 (1991).
[16] F. S. Pavone, F. Marin, P. De Natale, M. Inguscio, and F. Biraben, Phys. Rev. Lett. **73**, 42 (1994).
[17] C. J. Sansonetti, J. D. Gillaspy, and C. L. Cromer, Phys. Rev. Lett. **65**, 2539 (1990).
[18] P. Cancio Pastor, L. Consolino, G. Giusfredi, P. De Natale, M. Inguscio, V. A. Yerokhin, and K. Pachucki, Phys. Rev. Lett. **108**, 143001 (2012).
[19] X. Zheng, Y. R. Sun, J.-J. Chen, W. Jiang, K. Pachucki, and S.-M. Hu, Phys. Rev. Lett. **119**, 263002 (2017).
[20] R. J. Rengelink, Y. van der Werf, R. Notermans, R. Jannin, K. Eikema, M. Hoogerland, and W. Vassen, Nat. Phys. **14**, 1132 (2018).
[21] D. Shiner, R. Dixson, and V. Vedantham, Phys. Rev. Lett. **74**, 3553 (1995).
[22] R. Van Rooij, J. S. Borbely, J. Simonet, M. Hoogerland, K. Eikema, R. Rozendaal, and W. Vassen, Science **333**, 196 (2011).
[23] P. C. Pastor, G. Giusfredi, P. De Natale, G. Hagel, C. de Mauro, and M. Inguscio, Phys. Rev. Lett. **92**, 023001 (2004).
[24] P. C. Pastor, G. Giusfredi, P. De Natale, G. Hagel, C. de Mauro, and M. Inguscio, Phys. Rev. Lett. **97**, 139903(E) (2006).
[25] J. Derouard, M. Lombardi, and R. Jost, J. Phys. **41**, 819 (1980).
[26] P.-L. Luo, J.-L. Peng, J. Hu, Y. Feng, L.-B. Wang, and J.-T. Shy, Phys. Rev. A **94**, 062507 (2016).
[27] Y.-J. Huang, Y.-C. Guan, Y.-C. Huang, T.-H. Suen, J.-L. Peng, L.-B. Wang, and J.-T. Shy, Phys. Rev. A **97**, 032516 (2018).
[28] G. W. Drake, W. Nörtershäuser, and Z.-C. Yan, Can. J. Phys. **83**, 311 (2005).
[29] R. P. M. J. W. Notermans and W. Vassen, Phys. Rev. Lett. **112**, 253002 (2014).
[30] J.-L. Peng, H. Ahn, R.-H. Shu, H.-C. Chui, and J. Nicholson, Appl. Phys. B **86**, 49 (2007).
[31] A. Wienczek, K. Pachucki, M. Puchalski, V. Patkóš, and V. A. Yerokhin, Phys. Rev. A **99**, 052505 (2019).
[32] P.-L. Luo, J.-L. Peng, J.-T. Shy, and L.-B. Wang, Phys. Rev. Lett. **111**, 013002 (2013).
[33] P.-L. Luo, J.-L. Peng, J.-T. Shy, and L.-B. Wang, Phys. Rev. Lett. **111**, 179901(E) (2013).
[34] R. Li, Y. Wu, Y. Rui, B. Li, Y. Jiang, L. Ma, and H. Wu, Phys. Rev. Lett. **124**, 063002 (2020).
[35] C. J. Sansonetti, C. E. Simien, J. D. Gillaspy, J. N. Tan, S. M. Brewer, R. C. Brown, S. Wu, and J. V. Porto, Phys. Rev. Lett. **107**, 023001 (2011).